

phys. stat. sol. (b) **164**, 275 (1991)

Subject classification: 75.30, 75.40, S10.15

*Institute of Metal Physics, Academy of Sciences of the USSR, Ural Branch, Sverdlovsk<sup>1)</sup> (a)*  
*Institute of Inorganic Chemistry, Academy of Sciences of the USSR, Siberian Branch,*  
*Novosibirsk (b), and Institute of Physics, Academy of Sciences of Latvia, Riga (c)*

## Magnetic Phase Diagram of $(\text{Ni}_{1-x}\text{Mg}_x)\text{O}$ Solid Solutions

By

A. Z. MENSHIKOV (a), YU. A. DOROFEEV (a), A. G. KLIMENKO (b),  
 and N. A. MIRONOVA (c)

A magnetic phase diagram of the  $(\text{Ni}_{1-x}\text{Mg}_x)\text{O}$  solid solutions is drawn by the results of elastic magnetic neutron scattering and magnetic measurements. The ranges of homogeneous antiferromagnetism ( $0 \leq x \leq 0.37$ ), tricritical behaviour or frustrated antiferromagnetism ( $0.37 < x \leq 0.6$ ), cluster spin glass ( $0.6 < x \leq 0.75$ ) and paramagnetic behaviour of the  $\text{Ni}^{2+}$  spin moments in the ground state ( $x \geq 0.8$ ) are determined. It is shown that diamagnetic  $\text{Mg}^{2+}$  ions serve as a source of a random field inducing an extra diamagnetic moment of value  $0.35\mu_B$ .

Mit den Ergebnissen magnetischer Messungen und elastischer magnetischer Streuung von Neutronen wird ein magnetisches Phasendiagramm der  $(\text{Ni}_{1-x}\text{Mg}_x)\text{O}$ -Festkörperlösung angegeben. Die Bereiche für homogenen Antiferromagnetismus ( $0 \leq x \leq 0,37$ ), trikritisches Verhalten oder frustrierter Antiferromagnetismus ( $0,37 < x \leq 0,6$ ), Clusterspinglas ( $0,6 < x \leq 0,75$ ) und paramagnetisches Verhalten der  $\text{Ni}^{2+}$ -Spinmomente im Grundzustand ( $x \geq 0,8$ ) werden bestimmt. Es wird gezeigt, daß diamagnetische  $\text{Mg}^{2+}$ -Ionen eine Quelle für statistische Felder darstellen, die ein zusätzliches diamagnetisches Moment mit dem Wert  $0,35\mu_B$  induzieren.

### 1. Introduction

Magnetic systems under the conditions of destruction of the long-range magnetic order as a result of random substitution of one of the components in any sublattice have become of great interest. In general the problem of the destruction of magnetic order was reflected in the theorem of Imre and Ma [1]. According to this theorem any magnetically ordered state is unstable with respect to an arbitrary weak random field in a space with dimension  $n \geq 2$ . Different inhomogeneities of real systems may play the role of a random field. In particular, it may be a diamagnetic impurity as shown in [2].

The destruction of the long-range magnetic order as result of diamagnetic dilution was established in [3] on the example of  $(\text{Co}_{1-x}\text{Mg}_x)\text{O}$ . It was shown that at some magnesium concentration close to  $x \approx 0.5$  the topologically infinite antiferromagnetic cluster breaks into finite clusters the sizes of which were found from the broadening of antiferromagnetic coherent reflexes.

The present paper reports on the formation of random magnetic fields and the character of the destruction of long-range magnetic order on diamagnetic dilution for the  $(\text{Ni}_{1-x}\text{Mg}_x)\text{O}$  solid solutions. The  $(\text{Ni}_{1-x}\text{Mg}_x)\text{O}$  system represents a continuous set of solid solutions with NaCl-type crystal lattice. Here NiO is an antiferromagnet [4] with the wave vector  $k = 2\pi/a (1/2, 1/2, 1/2)$  and MgO is a diamagnet. It is known [5] that magnesium additions

<sup>1)</sup> Kovalevskaya 18, SU-620 219 Sverdlovsk, USSR.

permit the observation of the antiferromagnetic domain structure up to  $x \leq 0.37$ . However, according to the magnetic susceptibility measurements [6] the antiferromagnetic order exists in this system up to higher concentrations,  $x \leq 0.6$ . Above this concentration free  $\text{Ni}^{2+}$  ions and short-range antiferromagnetic order regions were observed by EPR spectroscopy [7].

In spite of available data about the magnetic properties of the  $(\text{Ni}_{1-x}\text{Mg}_x)\text{O}$  solid solutions the full magnetic phase diagram and the character of the phase transitions remain unclear. To elucidate this problem and to construct a complete magnetic phase diagram for the  $(\text{Ni}_{1-x}\text{Mg}_x)\text{O}$  solid solutions we investigated the magnetic state with elastic neutron scattering and SQUID magnetometry.

## 2. Experiment

The powdered samples were prepared by sintering of the initial NiO and MgO oxides and had the following compositions:  $x = 0, 0.1, 0.2, 0.3, 0.4, 0.5, 0.55, 0.6, 0.65, 0.7, 0.8,$  and  $0.9$ . According to the X-ray analysis all solid solutions had NaCl-type crystal structure with lattice parameter increasing linearly from NiO (0.4175 nm) to MgO (0.4211 nm). The powders were pressed into pellets of different thicknesses, 8 mm in diameter. The pellets were installed into a special container to obtain a sample  $\approx 50$  mm in length for neutron diffraction studies. For the magnetic susceptibility measurements a parallelepiped of  $2 \times 2 \times 5 \text{ mm}^3$  was cut out. Elastic neutron scattering was performed on a diffractometer mounted on the horizontal channel of the IVV-2M reactor in the temperature interval 4.2 to 600 K. A monochromatic neutron beam with the wave length  $\lambda = 0.181$  nm was produced by reflection from a germanium single crystal.

The magnetic susceptibility was measured in weak magnetic fields ( $\approx 1$  mT) with a SQUID magnetometer, the construction of which is described in detail in [8]. The long axes of the samples were oriented along the magnetic field. Temperature dependences of magnetic susceptibility were measured in the continuous regime with the sample fixed. For measurements we used the scheme typical for a study of spin glass. At first the sample was cooled in zero magnetic field down to 1.5 to 2 K, then a magnetic field was applied. During the first heating irreversible susceptibility ( $\chi_{\text{ZFC}}$ ) was measured. Reversible susceptibility ( $\chi_{\text{FC}}$ ) was measured on cooling after heating.

## 3. Experimental Results

### 3.1 Neutron diffraction studies

All the solid solutions up to  $x = 0.6$  have similar neutron diffraction patterns at 4.2 K with a magnetic reflection family with the forerunner reflection (1/2 1/2 1/2). Examples of the composition dependence of the (1/2 1/2 1/2) magnetic peak are displayed in Fig. 1. For  $x = 0$  to 0.4 the reflections have no detectable broadening and the intensity decreases smoothly with increasing  $x$ . Above this concentration the intensity decreases more rapidly and the width at half height is larger than for the samples with  $x < 0.5$ . Magnetic reflections are absent for the samples with  $x \geq 0.7$ . Analysis of the reflection intensities at 4.2 K and its temperature dependence (Fig. 2) allow us to find the average magnetic moment per atom ( $\bar{\mu}$ ) and the antiferromagnetic-paramagnetic transition temperatures ( $T_N$ ), respectively.

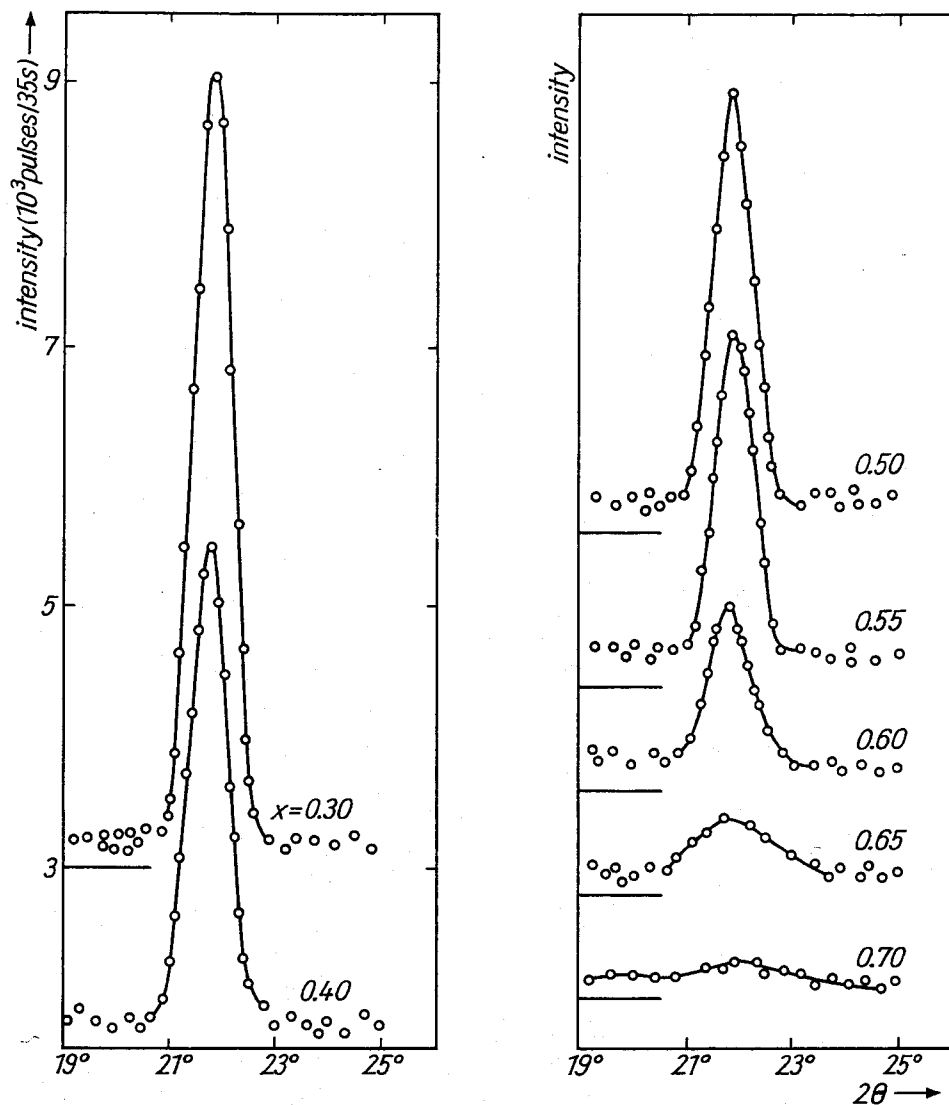


Fig. 1. The  $(1/2\ 1/2\ 1/2)$  magnetic reflections for the  $(\text{Ni}_{1-x}\text{Mg}_x)\text{O}$  solid solutions

### 3.2 Magnetic measurements

The temperature dependence of susceptibility for  $(\text{Ni}_{1-x}\text{Mg}_x)\text{O}$  with  $x \leq 0.6$  above 80 K was studied by Arkhipov [6] (insert in Fig. 3). Our measurements were made in the low-temperature range (up to 1.5 K) for samples with  $x \geq 0.5$  characterized by the destruction of long-range antiferromagnetic order.

Solid solutions with  $x = 0.6, 0.65,$  and  $0.7$  show irreversibility of magnetic susceptibility (Fig. 3). This effect disappears with decreasing  $x$ . Besides, the magnetic susceptibility for these samples does not break below  $T_N$  as is the case for usual homogeneous antiferromagnets (Fig. 3, 4). An increase of susceptibility below  $T_N$  was also observed for solid solutions with  $x = 0.55$  and  $0.5$  at low temperatures (Fig. 3). This results from the overlapping of the temperature dependences of two types of susceptibilities, one of which is characteristic of homogeneous antiferromagnets in which  $\chi(T)$  decreases below  $T_N$  and the other of paramagnets with the Curie-Weiss law.

Fig. 4 also shows the experimental  $\chi(T)$  data for solid solutions with  $x = 0.8$  and  $0.9$ . These samples have high values of susceptibility and fully obey the Curie-Weiss law.

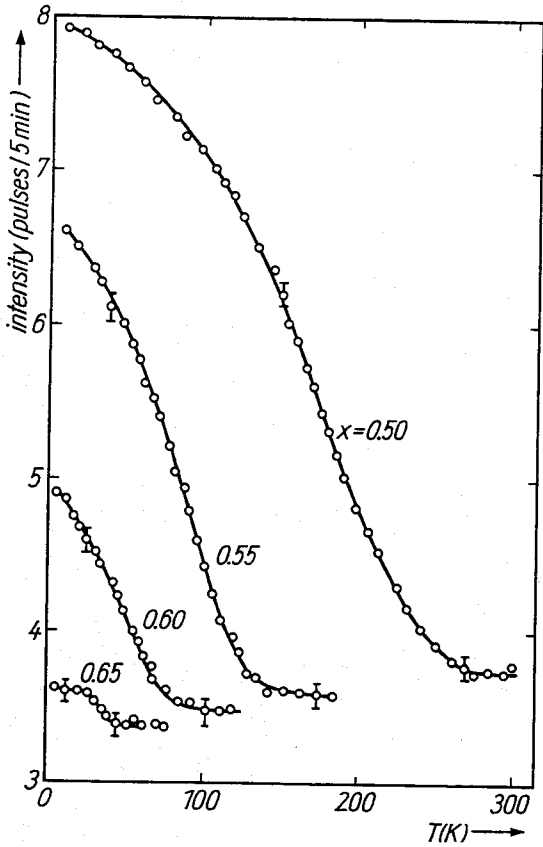


Fig. 2. The temperature dependence of the  $(1/2 \ 1/2)$  reflection intensity for some of the  $(\text{Ni}_{1-x}\text{Mg}_x)\text{O}$  solid solutions

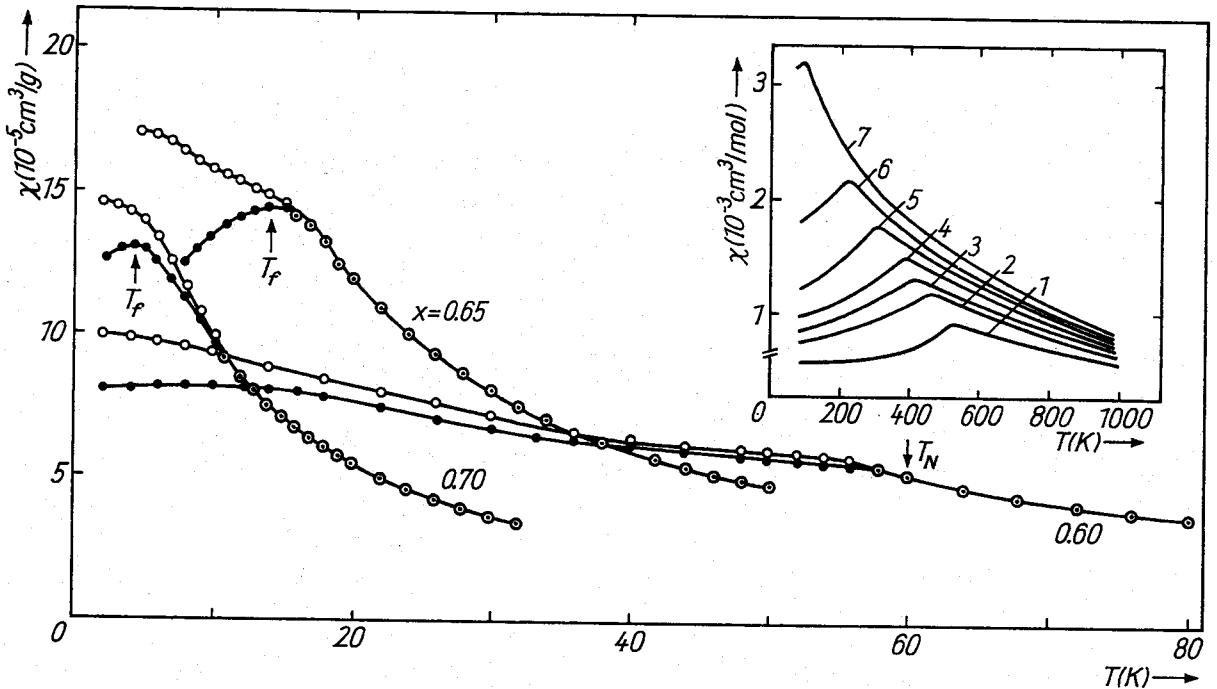


Fig. 3. Temperature dependence of the reversible (open circles) and irreversible (black points) magnetic susceptibility for  $(\text{Ni}_{1-x}\text{Mg}_x)\text{O}$  with different Mg contents. The transition temperatures  $T_f$  in a spin-glass state and  $T_N$  are marked by arrows. The insert shows  $\chi(T)$  for different  $x$ : (1) 0, (2) 0.1, (3) 0.2, (4) 0.3, (5) 0.4, (6) 0.5, (7) 0.6 [6]

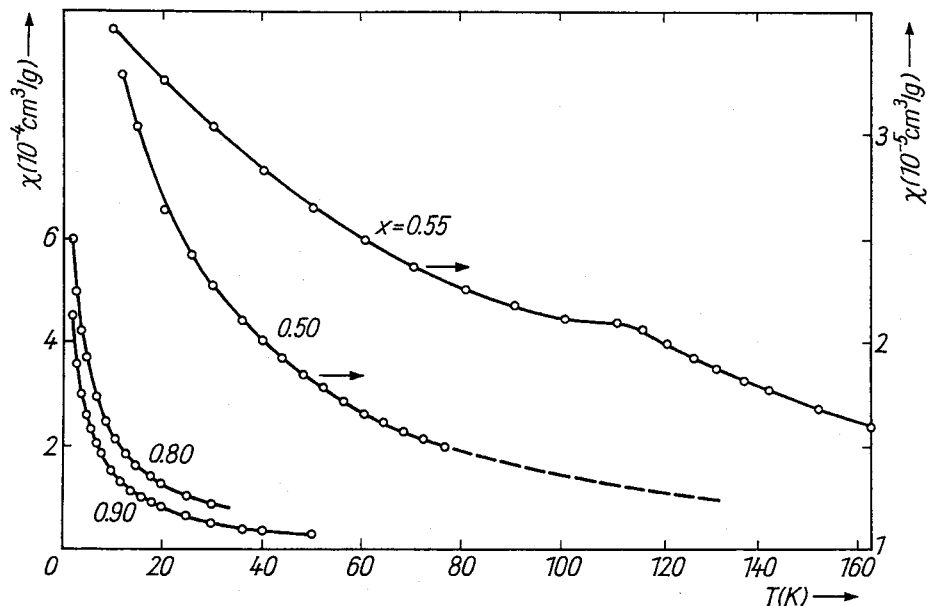


Fig. 4. The temperature dependence of the magnetic susceptibility for the  $(\text{Ni}_{1-x}\text{Mg}_x)\text{O}$  solid solutions with different  $x$

#### 4. Discussion

The magnetic phase diagram for the  $(\text{Ni}_{1-x}\text{Mg}_x)\text{O}$  solid solutions is drawn on the basis of the present experimental data (Fig. 5). It is characterized by four well-defined regions: homogeneous antiferromagnet ( $0 \leq x \leq 0.37$ ); tricritical behaviour or frustrated antiferromagnet ( $0.37 < x \leq 0.6$ ); cluster spin-glass ( $0.6 < x \leq 0.75$ ); and paramagnetic state of the  $\text{Ni}^{2+}$  ion spins ( $x \geq 0.8$ ).

##### 4.1 Homogeneous antiferromagnets

In the region corresponding to homogeneous antiferromagnets ( $0 \leq x \leq 0.37$ )  $T_N$  and  $\bar{\mu}$  decrease linearly with increasing  $x$ . Moreover, an antiferromagnetic domain structure is observed in this region. The temperatures of the domain structure are shown in Fig. 5 by crosses. Above these temperatures one can see a weak contrast due to a small rhombohedral deformation along the  $[111]$  direction.

Therefore, in the region of homogeneous antiferromagnets a topologically infinite cluster diluted by diamagnetic ions occurs. In this case the antiferromagnet-paramagnet phase transition temperature  $T_N$  is determined by the number of antiferromagnetically interacting ion pairs. The concentration dependence of the temperature  $T_N(x)$  may be found from the relation  $kT_N = E_{\text{ex}}^{(1)}$ , where  $E_{\text{ex}}^{(1)}$  is the exchange energy per magnetic atom and  $E_{\text{ex}}^{(1)}N(1-x) = E_{\text{ex}}$  is the total exchange energy,

$$E_{\text{ex}} = \frac{1}{2} NZ_{\text{ef}} J_{\text{ef}} S_{\text{ef}}^2 (1-x)^2. \quad (1)$$

Here  $Z_{\text{ef}}$  is the effective coordination number,  $J_{\text{ef}}$  the effective exchange integral,  $S_{\text{ef}}$  the effective spin of an  $\text{Ni}^{2+}$  ion.

Because of the antiferromagnetic structure with the wave vector  $\mathbf{k} = 2\pi/a (1/2, 1/2, 1/2)$  ferromagnetic and antiferromagnetic interaction between the nearest neighbours (NN) and antiferromagnetic coupling between the next nearest neighbours (NNN) occurs thanks to

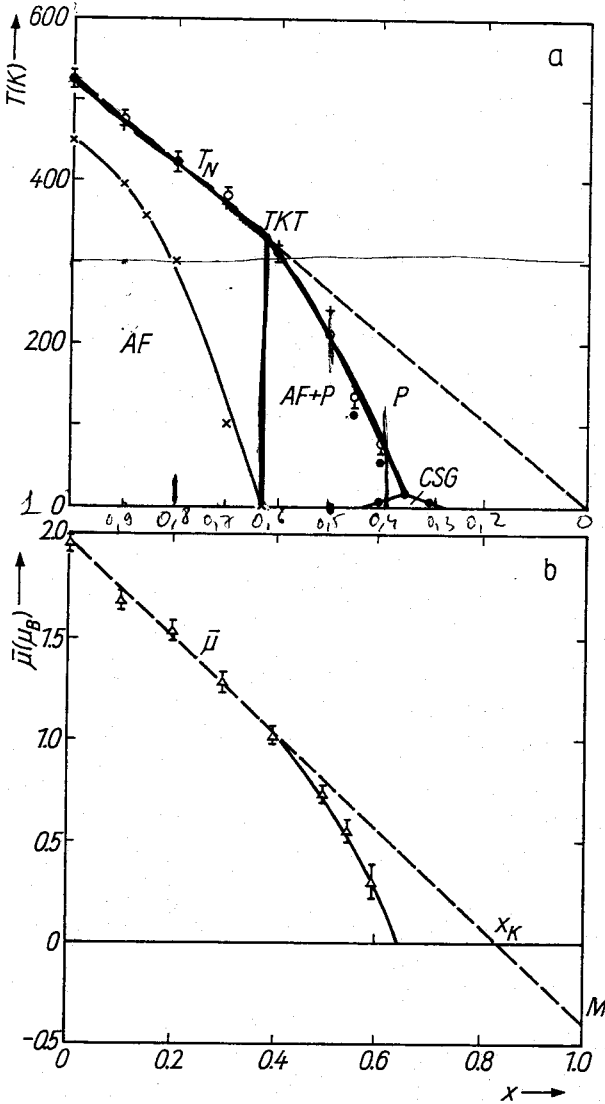


Fig. 5. a) The magnetic phase diagram and b) the concentration dependence of the average magnetic moment  $\bar{\mu}$  for  $(\text{Ni}_{1-x}\text{Mg}_x)\text{O}$ :  $\circ$ ,  $\Delta$  denote the present data obtained from the neutron diffraction measurements;  $\bullet$  the data obtained by SQUID magnetometry;  $+$  the data from [6];  $\times$  the temperatures up to which the antiferromagnetic domain structure was observed by Mironova et al. [5]. The dashed lines denote the second-order phase transition lines; the solid lines show the first-order phase transition lines

the intermediate position of the oxygen anions. In a first approximation we may neglect the rhombohedral distortion supposing that  $J_{\text{NNN}} \gg J_{\text{NN}}$ . Then  $Z_{\text{ef}} = Z_{\text{NNN}} = 6$ ,  $J_{\text{ef}} = J_{\text{NNN}}$ ,  $S_{\text{ef}} = S_{\text{Ni}}$ , and

$$T_{\text{N}} = \frac{1}{2k} Z_{\text{NNN}} J_{\text{NNN}} S_{\text{Ni}}^2 (1 - x). \quad (2)$$

The analogous expression for  $T_{\text{N}}$  obtained in the framework of a molecular field approximation [9] is as follows:

$$T_{\text{N}} = \frac{2Z_{\text{NNN}}}{3k} S(S + 1) J_{\text{NNN}} (1 - x). \quad (3)$$

Both expressions explain well the concentration dependence of  $T_{\text{N}}$  in the homogeneous antiferromagnet region (Fig. 5). Linear extrapolation of the experimental  $T_{\text{N}}(x)$  yields  $T_{\text{N}} = 0$  at  $x = 1$ . This implies that in this region  $J_{\text{MMM}} S_{\text{Ni}}^2 = \text{const}$ . Moreover,  $J_{\text{NNN}}$  and  $S_{\text{Ni}}$  are also constant. This follows from the small change of the  $(\text{Ni}_{1-x}\text{Mg}_x)\text{O}$  lattice parameter which increases approximately by 1% going from NiO to MgO. Assuming that the exchange

integral  $J_{\text{NNN}}$  is sensitive to this variation of the interatomic distance, it should decrease with increasing  $x$ . It follows from the magnetoelastic deformation of antiferromagnetic NiO as compression of the cubic lattice along the [111] direction. According to this assumption  $J_{\text{NNN}}S_{\text{Ni}}^2$  is constant when  $S_{\text{Ni}}$  increases with increasing  $x$ . However, from Fig. 5 it is seen that the average magnetic moment decreases more rapidly than follows from the law of magnetic moment mixture. Therefore, it is reasonable to suggest that the local magnetic moment of the  $\text{Ni}^{2+}$  ion also remains constant within the concentration range of the antiferromagnet.

Nevertheless, our experimental data on  $\bar{\mu}(x)$  do not obey the formula  $\bar{\mu}(x) = \mu_{\text{Ni}}(1 - x)$ . To describe the experimental  $\bar{\mu}(x)$  dependence in the homogeneous antiferromagnet region one should add a term. Then

$$\bar{\mu}(x) = \mu_{\text{Ni}}(1 - x) - Mx, \quad (4)$$

where  $M$  is the induced magnetic moment thermodynamically conjugated with a static magnetic field in the place of the magnesium ion. The value of  $M = -0.35\mu_{\text{B}}$  was determined by linear extrapolation of the experimental dependence  $\bar{\mu}(x)$  to  $x = 1$  (in Fig. 5b).

In fact the Mg ion in NiO should not be considered as a non-magnetic atom because of a static magnetic field formed due to rotation of the Mg electron orbit around the local molecular field created by the nearest environment of the nickel ions. In a general case this field is random both in value and direction because of different configurations of the nearest environment of the  $\text{Ni}^{2+}$  ion in a solid solution. However, in the homogeneous antiferromagnet region the random magnetic field connected with the Mg ions is broken only in the nearest neighbourhood. As a result the mean  $Z$ -projection of the Ni magnetic moments decreases with increasing  $x$  in the topologically infinite antiferromagnetic cluster.

#### 4.2 Tricritical region

The concentration  $x = 0.37$  is critical for breaking the infinite cluster into finite ones. Just for this concentration the antiferromagnetic domain structure disappears because of the weak rhombohedral distortion of a single crystal. The deviation of  $T_{\text{N}}(x)$  and  $\bar{\mu}(x)$  from linearity is caused by atomic spins which do not contribute both to the formation of exchange bond pairs and coherent neutron scattering. Therefore, we consider the point with the coordinates  $T = 525$  K and  $x_{\text{T}} = 0.37$  as tricritical. According to Landau theory [10] at this point in the  $T-x$  plane the line of the second-order phase transition transforms into two lines of first-order phase transitions. The region between these lines is characterized by the tricritical behaviour represented by a mixture of high-symmetry and low-symmetry phases which correspond in our case to the paramagnetic (P) and antiferromagnetic (AF) regions, respectively.

As a rule the reason of a tricritical point lies in the interaction between the vector and scalar order parameters [11]. In this case the thermodynamic potential is as follows:

$$\Phi = \Phi_0 + \frac{1}{2} A_1 l^2 + \frac{1}{4} C_1 l^4 + \frac{1}{2} A_2 u_{ik}^2 + \gamma l^2 u_{ik}, \quad (5)$$

where  $l = M_1 - M_2$  is the antiferromagnetic vector parameter,  $M_1$  and  $M_2$  are the sublattice magnetizations, and  $u_{ik}$  is the scalar order parameter. Here  $C_1 > 0$ ,  $A_2 > 0$ . The condition  $\partial\Phi/\partial u_{ik} = 0$  yields the renormalization coefficient  $C_1^* = C_1 - 2\gamma^2/A_2$  and allows to obtain  $C_1^* < 0$  which is the main condition for the appearance of a tricritical point (TKT).

In our case the scalar order parameter is the elastic rhombohedral distortion of the cubic NiO crystal. This parameter decreases with increasing Mg content up to  $x = 0.37$ . As a result, the antiferromagnetic system breaks into finite clusters with the typical size  $L$  the value of which decreases with increasing Mg content. From the broadening of the  $(1/2 \ 1/2 \ 1/2)$  reflection the cluster size was found to be  $L \geq 40 \text{ nm}$  for  $x = 0.6$  and  $L \approx 20 \text{ nm}$  for  $x = 0.65$ . For  $x > 0.65$  the cluster size becomes smaller than the coherent neutron scattering range ( $\approx 10 \text{ nm}$ ) and neutron diffraction reflections are absent.

We think that our measurements evidence the tricritical behaviour in the  $(\text{Ni}_{1-x}\text{Mg}_x)\text{O}$  solid solutions. The mixture of antiferromagnetic clusters and paramagnetic spins follows from the increasing magnetic susceptibility below  $T_N$  for the samples with  $x = 0.5$  to  $0.65$  and also from the observation of the magnetic susceptibility irreversibility at the Néel point (Fig. 3). Actually the strong increase of the magnetic susceptibility may be understood supposing that the total magnetic susceptibility represents the sum of two contributions,

$$\chi(T) = \chi_{\text{AF}}(T) + \chi_{\text{P}}(T),$$

where  $\chi_{\text{AF}}(T)$  is the temperature dependence of the antiferromagnetic cluster susceptibility which displays a common decrease of  $\chi(T)$  below  $T_N$  and  $\chi_{\text{P}}(T)$  is the Curie-Weiss temperature dependence of the paramagnetic spin susceptibility. Simultaneously the  $\chi(T)$  irreversibility at the Néel point for the samples with  $x \geq 0.6$  (Fig. 3) evidences a super-antiferromagnetic state of the solid solutions in which the cluster with an odd number of magnetic planes has different reaction to an external magnetic field depending on the pre-history of the sample.

#### 4.3 Cluster spin glass (CSG)

The system of small antiferromagnetic clusters in a paramagnetic matrix transforms into a spin-glass state below the temperature  $T_F$  corresponding to the maximum of  $\chi_{\text{ZFC}}$ . This temperature together with the cluster sizes decreases with increasing Mg content and for  $x > 0.8$  there are only antiferromagnetically interacting triplets and  $\text{Ni}^{2+}$  pairs in the ground state. This follows from the EPR experiments [7].

### 5. Conclusion

The present study of the magnetic phase diagram of the  $(\text{Ni}_{1-x}\text{Mg}_x)\text{O}$  solid solutions has thrown light on two very important physical phenomena:

- (i) diamagnetic impurity as the source of a random magnetic field;
- (ii) occurrence of a region of tricritical behaviour as a result of breaking the topologically infinite cluster into clusters with finite size  $L$ .

In our phase diagram of the  $(\text{Ni}_{1-x}\text{Mg}_x)\text{O}$  solid solutions the tricritical region is limited by two lines of first-order phase transitions. They are drawn according to the demands of theory. These lines show no evidence of hysteresis. However, the occurrence of magnetic susceptibility irreversibility at the Néel point as well as strong increase of susceptibility below  $T_N$  evidence the coexistence of antiferromagnetic and paramagnetic phases. This implies that the phase transition at  $T_N$  is not a cooperative process in these solid solutions. Due to the different volumes of antiferromagnetic clusters and their anisotropy the  $\text{P} \rightleftharpoons \text{AF}$  phase transition takes place in the temperature range  $\Delta T$  near some averaged  $T_N$  determined from the temperature dependence of magnetic coherent neutron scattering.



Thus, on the example of the antiferromagnetic NiO oxide diluted by diamagnetic Mg impurity it is shown that the character of the destruction of the long-range magnetic order depends on the influence of a random magnetic field.

### *Acknowledgements*

The authors would like to thank Yu. N. Skryabin for helpful discussions concerning the random fields and G. Gasnikova for the help in preparing the manuscript.

### **References**

- [1] Y. IMRE and S. MA, Phys. Rev. Letters **35**, 1399 (1975).
- [2] A. Z. MENSHIKOV, YU. A. DOROFEEV, A. G. KLIMENKO, and N. A. MIRONOVA, Zh. eksper. teor. Fiz. Pisma **51**, 640 (1990).
- [3] T. M. GIEBULTOWICZ, J. J. RHYNE, M. S. SEEHRA, and R. KAMRAN, J. Physique **49**, C8—1105 (1988).
- [4] W. L. ROTH, Phys. Rev. **110**, 1333 (1958).
- [5] N. A. MIRONOVA, A. T. BELYAEV, O. V. MILOSLAVSKAYA, and G. V. BANDURKINA, Ukrain. fiz. Zh. **26**, 848 (1981).
- [6] A. A. ARCHIPOV, Izv. Akad. Nauk Latv. SSR, Ser. fiz. tekhn. Nauk **3**, 24 (1981).
- [7] V. G. ANUFRIEV and U. A. ULMANIS, Izv. Akad. Nauk Latv. SSR, Ser. fiz. tekhn. Nauk, **5**, 113 (1979).
- [8] A. G. KLIMENKO, Preprint Inst. inorg. Chem., Siberian Branch, Akad. Nauk SSR, No. 85-1, Novosibirsk 1988.
- [9] M. V. MEDVEDEV and YU. N. SKRYABIN, phys. stat. sol. (b) **106**, K111 (1981).
- [10] L. D. LANDAU, Zh. eksp. teor. Fiz. **7**, 19 (1937).
- [11] A. Z. MENSHIKOV, Physica (Utrecht) B **149**, 249 (1988).

*(Received November 8, 1990)*